# Synchronous Inflation of a Valvuloplasty Balloon Catheter with Heart Rate: In-vitro Evaluation in Terms of Dilatation Performance

Junke Yao[1,2], Xinyi Pi[1], Giorgia Maria Bosi[1], Gaetano Burriesci[1,3], Helge Wurdemann[1]

***Abstract*— Balloon aortic valvuloplasty (BAV), a minimally invasive procedure to alleviate aortic valve stenosis, commonly employs rapid ventricular pacing (RVP) for balloon stabilization. However, the repeated and extended operation time associated with this technique poses potential complications. This paper introduces a novel approach to mitigate these concerns by employing a dilatation mechanism that is synchronized with the cardiac frequency, wherein the balloon catheter is fully inflated and deflated to a safe, low volume during the decrement of the ventricular pressure. The synchronized pacing was tested at a heart rate of 60 bpm. To experimentally validate the performance of this new approach, mock aortic roots reproducing different calcification patterns were used to compare the leaflets' mobility after the dilatation test with traditional BAV. Results confirm successful balloon pacing, maintaining low volume before the ventricular pressure increases. The dilatation performance assessment underscores that the proposed methodology resulted in a higher improvement in terms of the transvalvular pressure gradient and opening area. Optimal performance occurs at 60 bpm, yielding a 30.28% gradient decrease and a 21.35% opening area increase. This research represents a notable step forward toward the development of BAV devices capable of autonomous stabilization, eliminating the need for RVP and its related complications. Furthermore, the use of calcified aortic root (AR) phantoms contributes to an enhanced understanding of hemodynamic implications during BAV procedures.**

***Index Terms*— Valvuloplasty balloon catheters, synchronization device, balloon aortic valvuloplasty (BAV), aortic model, silicone phantoms**

## I. Introduction

Cardiovascular disease is a global health concern and remains the leading cause of death worldwide [1]. Aortic stenosis (AS) is a common form of heart valve disease that causes the blood flow to be restricted because the aortic leaflets grow stiffer and thicker, making it difficult for them to fully open [2]. Transcatheter aortic valve implantation (TAVI) is a minimally invasive intervention established as the preferred treatment option for severe AS in medium to high-risk patients [3]. Balloon Aortic Valvuloplasty (BAV) serves as a bridge treatment for TAVI, to pre-dilate the diseased valve [4]. During balloon inflation in BAV, the presence of pulsating blood ejection and heart contractions can introduce instability to the inflated balloon, potentially leading to malposition, tissue damage, or cardiac arrest [5], [6]. To oppose this effect, rapid ventricle pacing (RVP) is employed to temporarily reduce cardiac output and keep the balloon stable. However, RVP is associated with several potential complications, such as transient hypotension during balloon inflation, which may have adverse clinical impact [7]. Recent research has focused on improving balloon catheter design to avoid RVP by proposing non-occlusive balloon catheters or multi-compartment balloon catheters [8], [9]. However, incomplete dilation and significant backflow from the aorta to the left ventricle via the large central orifice of these balloon catheters induce significant changes in physiological flow and energetic losses. A prior study explored an alternative solution for balloon stabilization during cardiac cycles through self-inflation and deflation procedures [10]. This approach resembles intra-aortic balloon pump (IABP) control but necessitates balloon expansion to fracture calcification and reopen heart leaflets. Therefore, it is necessary to design a setup for balloon inflation synchronized with the heartbeat and evaluate the pattern of the inflation procedure for this method with expected dilatation results.

The main goal of this study is to analyze the phase synchrony of balloon inflation with cardiac frequency using a robotic device and assess its dilatation performance compared to the standard. To achieve this, the balloon fully inflated and deflated to a safe, low volume during the ventricular pressure decrement phase using the signal from a pressure transducer to monitor the ventricular pressures. We hypothesize that synchronized balloon inflation based on blood pressure during the BAV technique will yield equivalent or improved dilatation performance while maintaining balloon stability during systole. To validate this hypothesis, silicone aortic root models with stiffened wax patterns mimicking calcification were used to check the dilatation results under different inflation speeds and numbers of pacing cycles, compared with maintaining a fully inflated balloon during the cardiac cycle. By exploring this novel approach, we hope to contribute to the development of improved balloon catheter techniques that can enhance the safety and efficacy of balloon aortic valvuloplasty procedures.

## II. Automatic Balloon Inflation System

Clinically, during BAV, a balloon catheter is inserted through the vessel, across the valve, and towards the aortic root. Prior to the dilatation, RVP is applied to increase the

Manuscript received: 15 Jul 2024; Revised: 17 Nov 2024; Accepted: 16 Dec 2024.

This paper was recommended for publication by Editor Yong-Lae Park upon evaluation of the Associate Editor and Reviewers' comments.

[1]J. Yao, X. Pi, G.M. Bosi, G. Burriesci, H. Wurdemann are with the Department of Mechanical Engineering, University College London, UK. h.wurdemann@ucl.ac.uk

[2]Junke Yao is with the Department of Engineering, King's College London, UK.

[3]Gaetano Burriesci is the group leader of Bioengineering at Ri.MED Foundation, Palermo, Italy. g.burriesci@ucl.ac.uk

Digital Object Identifier (DOI): see top of this page.

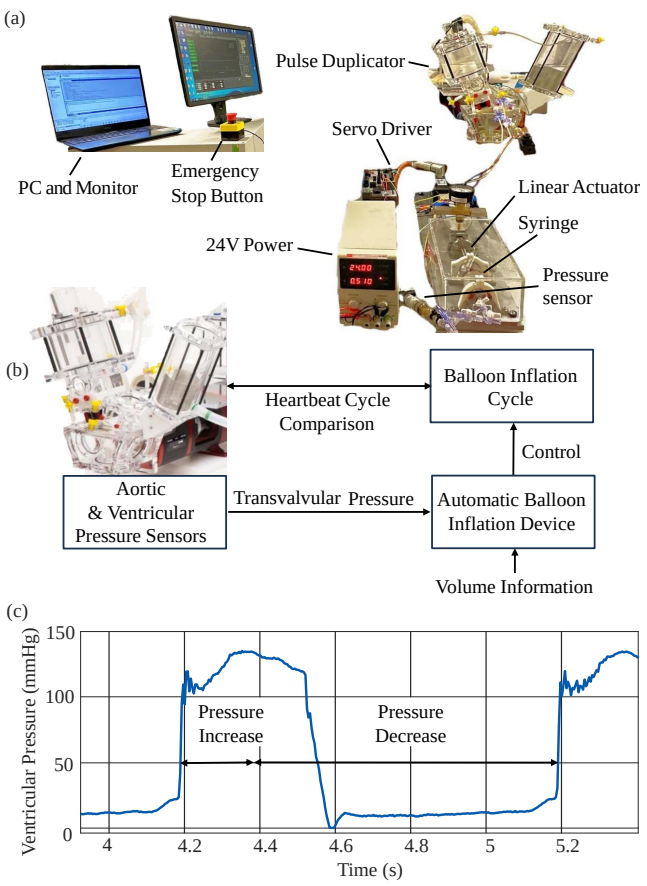


Fig. 1. (a) The picture of the experimental setup for ABID connecting to the pulse duplicator; (b) The flowchart of communication between ABID and the pulse duplicator to achieve the balloon synchronization; (c) One cardiac cycle of ventricular pressure with defined pressure increase and pressure decrease duration at 60 bpm heart rate, where the balloon pacing within the pressure decrease duration.

heart rate to 180-200 bpm to achieve balloon stability [11]. Two to three balloon inflations are conducted to ensure the correct position and effective dilating [12]. The balloon is manually inflated by injecting a saline solution with a syringe connected to a manometer. The pump-in action is stopped once the internal pressure reaches the balloon's nominal pressure value or the volume of the ejected solution reaches the nominal volume. Streamlining this process to synchronize balloon inflation with the heartbeat could potentially eliminate the need for RVP. Hence, the creation of an inflation device is essential to realize this concept.

An automatic balloon inflation device (ABID) employed in this work was designed for the controlled inflation of a balloon catheter with a user-defined rate and volume. A Kollmorgen AKD-T00606 BASIC drive controls a Kollmorgen AKM22G-ANDNC-00 servo motor(Altra Industrial Motion, Braintree, MA, USA) which is coupled with a linear actuator (PC25LX999B03-0100FM, Thomson, Kristianstad, Sweden) for pushing the plunger of a 50 ml gas-tight syringe. The syringe is used to inject the solution into the balloon, which is covered by a safety transparent box. To prevent the balloon from being inflated over the burst pressure, a PXM319-007A10V pressure transducer is hydraulically linked to the balloon catheter. The phase delay for the low-pass filter in the driver used for processing the real-time pressure signals is approximately 30 microseconds, which is negligible given the 60 bpm heartbeat. The drive optimizes the motor performance via a computer interface software AKD Workbench. Users can control the speed rate, the number of inflation or deflation procedure cycles, and the amount of the injected or withdrawn solution fluid. ABID connected with a pulse duplicator is shown in Fig. 1(a).

A system was created to connect the pulse duplicator and ABID to transfer pressure data and control ABID by the pulse duplicator to synchronize balloon inflation with the cardiac cycle, as shown in Fig. 1(b). A pressure sensor (XMLP500MC71F, Telemecanique, Switzerland) was hydraulically connected to the ventricular chamber of a Vivitro Pulse Duplicator (ViVitro Labs, Inc. Victoria, BC, Canada). The ViVitest software enables the analysis of the flow rate and pressures of the aortic and ventricular chambers and the estimation of the effective orifice area. The flow pressure signal at the ventricular chamber is transmitted to ABID, synchronized with the cycle of balloon inflation and deflation. The actuator's real-time position, translated into the internal volume of the balloon, and the ventricular pressure are recorded and used to validate synchronization. The balloon is inflated to dilate the calcified aortic leaflets immediately after the closing phase begins and is deflated before the opening phase. During the sudden systolic increase in ventricular pressure, the balloon remains at a low volume to maintain stability. As the pressure begins to decrease, the balloon undergoes a controlled inflation and deflation cycle, ensuring the effective dilatation of the calcified leaflets. The device detects heart rates over five consecutive cycles, and the inflation and deflation speeds are adjusted based on the average heart rate from these cycles. In cases where heart rates fluctuate, the inflation and deflation speeds are dynamically modified to align with the variations in the heart cycle, ensuring consistent synchronization.

Fig. 1(c) shows a ventricular pressure waveform generated by the pulse duplicator during testing. The onset of pressure increment is defined as the point at which the pressure begins to rise steeply. The beginning of pressure decrement, which marks the instant the syringe starts moving, is determined following the maximum pressure value, characterized by the second peak with a slightly increasing slope, followed by a slightly declining slope. The initial peak is excluded since a sustained decrease does not follow it in pressure. The inflation and deflation speed are synchronized with the pressure decrement duration to ensure the balloon catheter only expands within the low ventricular pressure to keep itself stable. The motion sequences of the plunger and data capture from the pressure transducers were controlled and synchronized in a purposely developed environment in the AKD Workbench software to program ABID. The synchronization mechanism enables the syringe plunger to move between two specified positions, serving as the upper and lower limits of the balloon volume values. During pressure increment, the balloon maintains a lower volume, and its

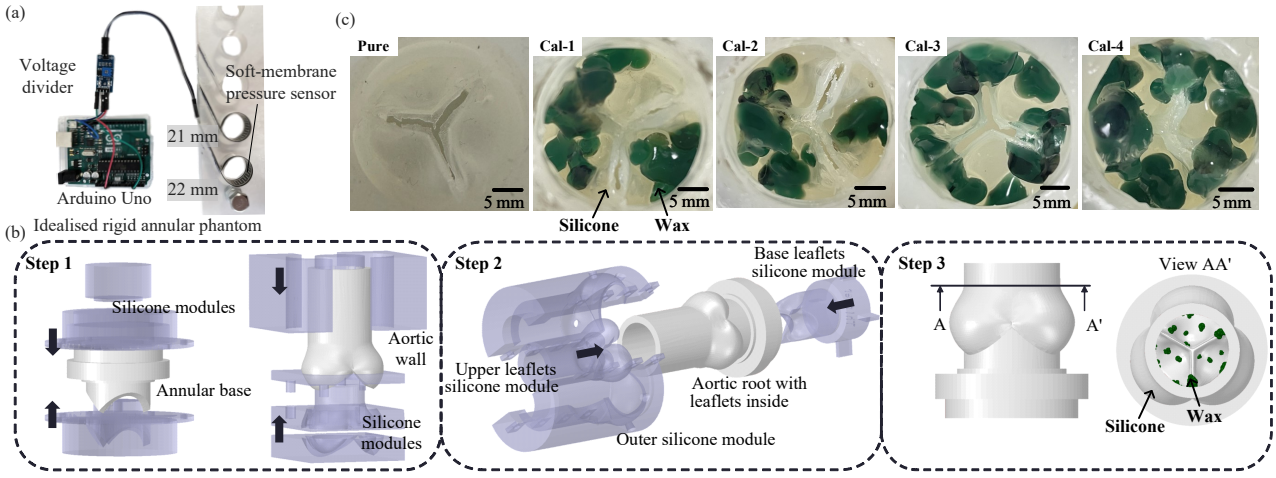


Fig. 2. (a) 21 and 22 mm rigid annular phantom with pressure sensors inserted inside and connected to Arduino Uno to collect data; (b) The three steps for creating the silicone aortic root phantoms (white) with wax drip (dark green) as calcification on the leaflets; (c) One pure silicone phantom and four calcified silicone aortic root phantoms (Cal1 to Cal4) up views, where the transparent region is silicone polymer, and the dark green region is wax.

inflation commences at the onset of pressure decrement.

## III. Aortic Root Models for Dilatation Assessment

### A. Rigid phantoms

The radial force applied by the balloon during its inflation procedure can be used as a factor for comparing the different dilatation performances between traditional balloon inflation and balloon pacing inflation. Therefore, rigid idealized aortic annular phantoms were created to measure the pressure applied by the expanded balloon. For the 23 mm balloon, these phantoms were 21 mm and 22 mm. A thin, soft membrane pressure sensor (RP-LL-110, FSR402 pressure sensor, RunesKee, China) features an axial length of 15 mm. Fig. 2(a) depicts the placement of the thin soft-strip pressure sensor inside the rigid phantom. This was connected to an Arduino Uno board via a voltage divider to record the pressure signals during the balloon expansion of the annular phantoms. The soft-strip pressure sensor measures the pressure range within 0.002 to 0.934 atm.

### B. Silicone calcified phantoms

Assessment of aortic stenosis severity involves measuring several criteria parameters such as the mean transvalvular pressure gradient, the pressure difference between the ascending aorta and the left ventricular outflow tract (LVOT), and the effective orifice area (EOA), which represents the mean minimal cross-sectional area of the flow jet during systole. The progression of calcified AS is associated with an increase in blood flow acceleration and mean pressure gradient due to the gradual area reduction. Hence, the diagnosis of AS is confirmed by a thickened aortic valve with a restricted opening area and a high mean gradient [13].

The performance of different inflation procedures in dilating the calcified aortic valve can be evaluated based on the mean systolic transvalvular pressure drop [14]. Silicone AR phantoms were created for this purpose, using silicone as the material for both the aortic wall and valves. The aortic wall and LVOT base were created separately using silicone material Dragon Skin 20 (Smooth-On, Inc. Macungie, PA, USA), as shown in Fig. 2(b) step 1. The ascending aortic wall with Valsalva's sinuses and the holder for inserting the aortic root model into the pulse duplicator was created by silicone casting. Then, these two parts were connected by modules, and the leaflets inside were created by injecting silicone from Dragon Skin 10, as shown in step 2. Wax was utilized to replicate calcification, which is rigid and fragile. The aortic wall was shortened to facilitate easy dripping of the wax onto the leaflets. The wax was dispersed on the leaflets in a random pattern with approximately equal weight and subsequently covered by a thin layer of silicone membrane to prevent the broken wax from flowing into the pulse duplicator in Fig. 2(b) step 3. In TAVI procedures, operators typically select a balloon that is up to 10% larger than the annular diameter [15]. In this study, a 23 mm balloon catheter was chosen, which is appropriate for annular diameters of 21 mm. The idealized aortic root models with 21 mm annular dimension are shown in Fig. 2(c), where the four aortic root phantoms are with calcification (Cal1, Cal2, Cal3, Cal4). There are two levels of calcification, where Cal1 and Cal2 have the same wax distribution on three leaflets' belly and one commissure spanning two cusps, representing mild calcification. Cal3 and Cal4 represent severe calcification, as all leaflets and commissures are stiffened with wax.

## IV. Experimental Study

### A. Synchronization Validation

To ascertain the synchronization of balloon catheter inflation with the cardiac cycle, we employed a pulse duplicator system connected to the inflation device. This machine accurately replicates the function of the heart and enables the measurement of the fluid pressure at various chambers. The ABID was controlled by the left ventricular chamber pressure, ensuring a realistic simulation of the pacing mechanism. To prevent possible damage to the pulse duplicator,

the balloon catheter was initially placed outside the pulse duplicator as a preliminary pacing validation.

Before the intervention procedure, patients are instructed to assume a supine position, which promotes relaxation and maintains the heart rate at a mean resting frequency of about 60 bpm [16]. Therefore, a heart rate of 60 bpm was chosen during the balloon pacing dilatation experiment, which typically corresponds to a duration of approximately 30% of the cardiac cycle [17]. The cardiac output level was set to 5 L/min, and the mean aortic pressure was set to 100 mmHg. Based on previous studies, the low 'safe' volume of the 23 mm balloon catheter is determined to be approximately 10 ml [10]. During the experiment, the balloon is first inflated to 10 ml at a slow flow rate of 1 ml/s. Subsequently, the balloon is pumped between 10 ml and 21 ml. The flow rate for balloon inflation is calculated based on the heart rate, the ratio of systole to diastole, and the volume for injecting and withdrawing. The average pressure decrement and cycle duration of five cycles were calculated by detecting the start of ventricular pressure decrement duration as shown in Fig. 1(c). A safety margin (3 ml/s) is incorporated into the calculated flow rate to prevent the balloon from being unable to be deflated to the low volume at the beginning of the pressure increment. The experimental protocol was conducted according to the following steps:

1) A mechanical valve was implanted in the aortic valve position, and the pressure sensor was connected hydraulically to the ventricular pressure, feeding the ventricular pressure signal to the ABID.
2) The desired heartbeat value was set, with a cardiac output of 5 L/min and a mean aortic pressure of 100 mmHg.
3) The balloon inflation and deflation process was initiated when the ABID detected the start of ventricular pressure decrement. The balloon was inflated, enforcing the defined flow rate, and, subsequently, deflated to the low 'safe' volume using the same flow rate.
4) This inflation and deflation process was repeated 10 times, after which the balloon was fully deflated.
5) The pump of the pulse duplicator was stopped in preparation for the next heartbeat value.

Three tests were conducted for each heartbeat value. The recorded data, including balloon volume and ventricular chamber pressure, were imported into Matlab for further analysis. This data analysis aimed to assess the synchronization between the pulse duplicator and the balloon pacing.

### *B. Dilatation Performance Comparison*

The variation in balloon catheter inflation techniques can lead to diverse operational outcomes in terms of dilatation. Consequently, the novel pacing action of the balloon may influence the dilatation performance, warranting a comparison between traditional balloon inflation and quick pacing. To facilitate this comparison, two distinct aortic root phantoms, rigid and silicone, were employed. These phantoms were utilized to assess the balloon's dilatation performance based on factors such as radial force, the opening area of the dilated aortic root phantom, and pressure drop experienced by the flow as it traversed the calcified valve.

*1) Radial Pressure Assessment within Rigid phantoms:* During the BAV procedure, the balloon catheter dilatation protocol typically involves a single inflation lasting approximately 30 seconds, and the balloon is kept fully inflated for about 4 to 6 seconds [4], [18]. It is recommended to repeat this inflation procedure at least three times to achieve the desired dilatation effect [19]. Therefore, following the provided clinical guideline, the balloon catheter underwent inflation at a rate of 0.7 ml/s for 30 seconds. Following a 5-second inflation period, the balloon was deflated using the same flow rate. This inflation and deflation procedure was performed by inserting the balloon catheter inside two rigid phantoms, which were attached with thin pressure sensors. Five tests were performed, and the results were averaged. During balloon pacing dilatation, the high inflation speed used for synchronization purposes carries the risk of balloon rupture, especially when employed inside a rigid phantom. To mitigate this risk and investigate the relationship between the speed and the pressure of the balloon expanding the rigid phantom, different ejection flow rates were utilized for balloon inflation and deflation. Specifically, flow velocities of 6 m/s, 8 m/s, 10 ml/s, and 12 m/s were selected for the inflation and deflation cycles during the pacing process. Each dilation procedure involved 10 pacing cycles.

*2) Pressure Drop Assessment of Silicone Phantoms:* For the study, four silicone phantoms with two levels of calcification were employed to simulate both traditional balloon dilatation and pacing dilatation procedures. These phantoms allowed us to assess and compare the performance of the balloon catheter under different dilatation techniques. Before conducting the dry dilatation experiments, the silicone phantoms were tested in the pulse duplicator to assess the opening area and pressure gradient of the valve, thereby evaluating its functionality before balloon expansion. The silicone calcified aortic root phantoms were inserted into the pulse duplicator, and standard operating conditions were applied: 60 bpm with a cardiac output level of 5 L/min and mean aortic pressure of 100 mmHg. Employing the ViViTest software within the pulse duplicator, we assessed pressure drop due to the stiffer valve and calculated the EOA. Subsequently, the dry dilatation procedures were performed on the silicone phantoms using two distinct balloon expansion protocols similar to those employed with the rigid phantoms. Cal1 and Cal3 underwent traditional balloon inflation three consecutive times, while Cal2 and Cal4 underwent ten cycles of fast balloon inflation at speeds corresponding to 60 bpm calculated in the synchronization experiment. Following the dilatation procedures, the phantoms were reintroduced into the pulse duplicator to measure the parameters under the same cardiac conditions. These measurements were utilized to compare the performance of the two different balloon catheter dilatation techniques.

## V. Results and Discussion

### A. Balloon Dilatation Synchronization

The experimental procedure involved the inflation and deflation of a balloon catheter within a range of 10 to 21 ml, positioning the balloon adjacent to the mock silicone ventricle to facilitate comparative analysis of its contractile and relaxation states. The volume of the balloon was quantified based on the plunger position. The balloon inflation flow rate was evaluated based on an averaged calculation across a heart rate of 36.00 ml/s at 60 bpm. In the context of Fig. 3, the balloon volume and ventricular pressure data were plotted during the balloon pacing process. The grey region corresponds to the ventricular pressure increment phase, during which the balloon volume remained constant at 10 ml. Three specific instances of balloon pacing were captured in the depicted images: start at 10 ml, mid-diastole at 21 ml, and end-diastole at 10 ml. The outline of the silicone left ventricle is delineated by a red dashed line for visual clarity.

### B. Dilatation results

The balloon inserted inside 21 and 22 mm rigid annular phantoms are shown in Fig. 4(a), where it is inflated totally with 21 ml saline solution inside, and the balloon inside the 21 mm phantom becomes gourd-shaped. The pressure applied from the balloon to the inside of the 21 mm rigid annular phantom is shown in Fig. 4(b), where the pressure increases to 0.7 atm when the balloon is completely inflated and then decreases to 0.6 atm within the completed inflated duration. The nominal pressure for the balloon is 4 atm when inflated with 21 ml of the saline solution under free inflation. Considering that the internal pressure of the balloon during inflation almost reaches 6 atm (its burst pressure), the pacing balloon inflation test is not conducted within the 21 mm phantom to prevent the balloon from bursting. Fig. 4(c) displays the pressure exerted by the balloon on the interior of the 22 mm rigid annular phantom during both traditional inflation and pacing inflation procedures. For traditional inflation, the pressure reaches a peak of 0.0866 atm during full inflation and then stabilizes at 0.0860 atm. During pacing inflation, the pressure exhibits spikes, with the frequency increasing as the flow rate increases. Notably, the peak pressure value of the spikes remains consistent over ten cycles of pacing. At flow rates of 6 ml/s and 8 ml/s, the peak pressure reaches 0.0866 atm, which is similar to the pressure observed during traditional inflation. In addition, at flow rates of 10 ml/s and 12 ml/s, there is a notable increase in pressure, jumping to 0.0894 atm.

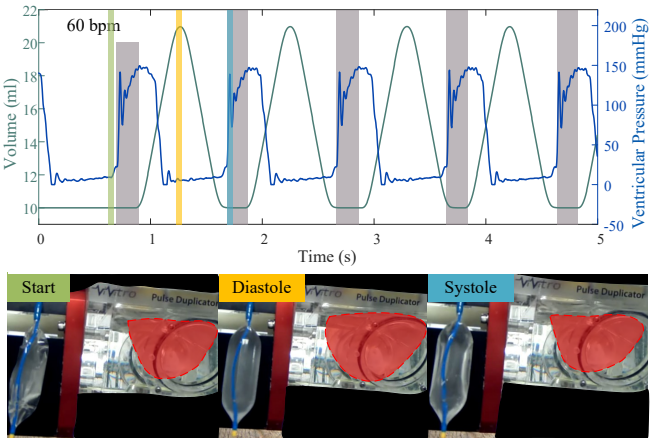


Fig. 3. The balloon catheter volume and ventricular pressure data plots under 60bpm heartbeat with the pressure increasement duration region covered by grey and the balloon status at the start (green), diastole (yellow), and systole (blue) of the silicone left ventricle of the pulse duplicator, all of which happen during the time are demonstrated in the time scale plot. The red region covers the silicone left ventricle during the cardiac cycle at the time of three balloon status.

All pure silicone phantoms used for wax attachment result in consistent values of the transvalvular pressure gradient (TPG) of all in the range from 8 to 10 mmHg and consistent estimates of the EOA, which remains in the range from 2.60 $cm^2$ to 2.70 $cm^2$. The criteria to identify the severity of aortic stenosis are a mean pressure gradient larger than 40 mmHg and an EOA less than 1 $cm^2$ and the health valve case is identified as a mean pressure gradient less than 10 mmHg or an EOA larger than 3 $cm^2$ [20], [21]. Less wax drips in Cal1 and Cal2 result in TPG around 41 mmHg and mean EOA of 1.25 $cm^2$, while more wax drips in Cal3 and Cal4 result in TPG range within 58.5 to 61 mmHg and mean EOA of 0.93 $cm^2$. The two wax distributions producing the most severe AS were tested for two different dilatation methods. One example of the procedure of the balloon catheter dilating the calcified AR phantom is demonstrated in Fig. 4(d), where the balloon is inserted anterogradely.

The graphs in Fig. 4(e) illustrate measurements of aortic and ventricular pressure ($P_v$ and $P_a$ represent the fluid pressure in the aortic chamber and ventricular chamber, respectively) at the aortic valve for various calcified aortic root phantoms. Before and following dilatation (indicated by dashed lines), the pressure differences are depicted. Specifically, the dark blue and dark green lines represent ventricular pressure for Cal1 and Cal3 during traditional inflation, while blue and green lines represent ventricular pressure for Cal2 and Cal4 during balloon pacing inflation at 60 bpm. The red lines denote aortic pressure for all phantoms before dilatation, with the dashed line indicating post-dilatation. All of the ventricular pressure showed a marked decrease during the systole after ballooning, as summarised in Table I. For the traditional dilatation procedure, the TPG of Cal1 reduced from 41.23 mmHg before the dilatation to 35.03 mmHg after the procedure (15.04% reduction). The TPG of Cal3 reduced from 58.71 mmHg before to 48.71 mmHg after the procedure (17.03% reduction). For balloon pacing at 60 bpm, in Cal2, the procedure reduced the TPG from 41.01 mmHg to 29.90 mmHg (27.09 % reduction); and for Cal4, from 60.74 mmHg to 42.33 mmHg (30.28 % reduction). Calculation of the EOA in Fig. 4(f) was performed through Gorlin's equation, as requested in the ISO 5840 [22]. The baseline silicone phantom exhibited an EOA of approximately 1.98 $cm^2$. The EOA before dilation, corresponding to gradual inflation and heart rate at 60 bpm, is reported in Table I. The maximum increase of the area after dilatation is Cal4 for balloon pacing

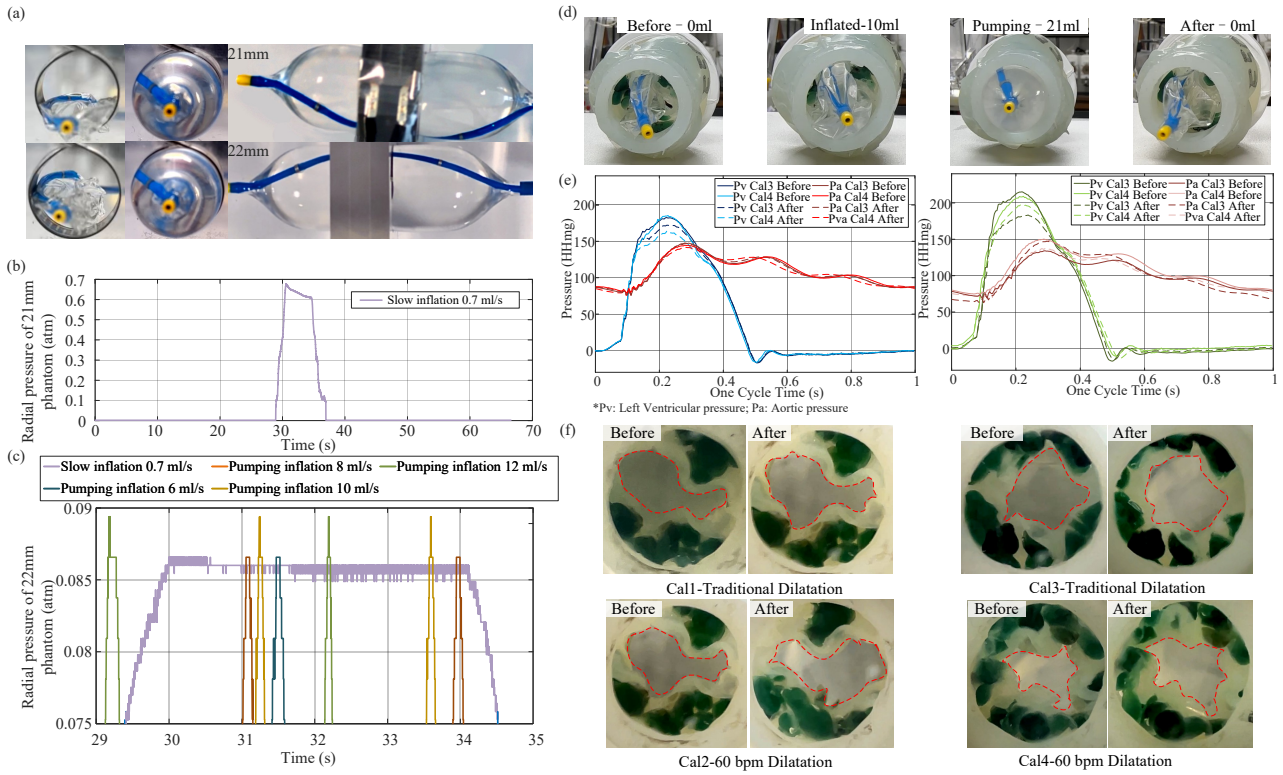


Fig. 4. Dilatation results for rigid phantoms in (a), (b) and (c); for silicone phantoms in (d), (e) and (f). (a) The front views of the fully deflated balloon and the front and side views of the fully inflated balloon inside the 21 and 22 mm rigid phantom; (b) The expanding pressure when the balloon is slowly inflated inside the 21 mm rigid phantom; (c) The expanding pressure when the balloon is slowly inflated and pacing inside the 22 mm rigid phantom; (d) The procedure for balloon catheter dilatation inside silicone phantoms; (e) The aortic and ventricular pressure ($P_a$ and $P_v$) plots for traditional inflation and balloon pacing within the calcified aortic valve phantoms, where the mean aortic pressure is 100 mmHg for all aortic pressure curves, and Cal1 and Cal3 for the traditional and Cal2 and Cal4 for the pacing at 60 bpm; (f) The opening leaflets of the calcified aortic root inside the pulse duplicator under two procedures before and after the balloon dilatation including traditional inflation, pacing dilatation under 60bpm.

TABLE I

PERFORMANCE FOR TRADITIONAL AND PACING DILATATION PROCEDURES

| | Before Dilatation | | | | After Dilatation | | | |
|---|---|---|---|---|---|---|---|---|
| | Traditional-Cal1 | 60bpm-Cal2 | Traditional-Cal3 | 60bpm-Cal4 | Traditional-Cal1 | 60bpm-Cal2 | Traditional-Cal3 | 60bpm-Cal4 |
| Transvalvar Pressure Gradient [mmHg] | 41.23 | 41.01 | 58.71 | 60.74 | 35.03 (15.04%) | 29.90 (27.09%) | 48.71 (17.03%) | 42.33 (30.28%) |
| Effective Orifice Area [$cm^2$] | 1.23 | 1.27 | 0.96 | 0.89 | 1.36 (10.60%) | 1.50 (18.11%) | 1.07 (11.46%) | 1.08 (21.35%) |

*The values are the average of 10-cycle recording results.

at 60 bpm (0.89 to 1.08 $cm^2$ with 21.35% improvement), and the most modest enhancement is for Cal1, for the traditional inflation (1.23 to 1.36 $cm^2$ with 10.60%).

### C. Discussion

The present study introduces an innovative synchronization mechanism for balloon catheter dilatation, realized through an automated balloon inflation device. This system is engineered to compute the prevailing average heart rate and discern the commencement of ventricular pressure increment and decrement, thereby achieving synchronized balloon pacing in harmony with the cardiac cycle. Additionally, the system calculates the appropriate inflation and deflation rates, ensuring the balloon is at low volume during the ejection phase, allowing blood pumping, and achieving dilatation during diastole, contributing to the arrest of the regurgitate flow. The research seeks to evaluate the viability of this pacing strategy in the context of BAV, comparing its dilatation efficacy against traditional inflation techniques. This comparison is based on parameters such as radial pressure and the improvement of the calcified leaflets. The results with phantoms mimicking typical calcification patterns indicated that the proposed approach could outperform the traditional inflation procedure in terms of TPG and EOA percentage increments, underscoring the potential advantages of the proposed synchronization-driven pacing methodology.

RVP constitutes a required procedural component in cardiac interventions utilizing balloon catheters, notably in TAVI and BAV. Its purpose is to temporarily curtail cardiac output, thereby ensuring balloon stability during blood ejection. Nevertheless, findings from clinical investigations have underscored the potential drawbacks of frequent RVP instances

and prolonged RVP durations. These include unfavourable outcomes, encompassing both short-term and enduring mortality effects [7], [23]. In light of these observations, the minimization of rapid ventricular pacing occurrences is advocated to optimize patient outcomes and mitigate potential adverse consequences, especially in patient cohorts susceptible to acute kidney injury and associated risks. An effective approach to mitigate the necessity for frequent RVP utilization involves circumventing balloon occlusion during systole and ensuring sufficient cardiac output throughout the procedure. This concept aligns with the deployment of a mechanical support device known as an IABP, which operates by inflating immediately after the closure of the aortic valve and deflating during diastole [24]. In the present investigation, a commercially accessible valvuloplasty balloon catheter was repurposed as a pacing balloon. It functioned in synchrony with the cardiac output, triggered by blood pressure dynamics. The synchronization results show the balloon pacing at a heart rate of 60 bpm, achieving successful inflation of the balloon during low ventricular pressure, maintaining the balloon at a 'safe' volume (10 ml) [10], [25]. The minimal pacing speed of the balloon, as the inflation and deflation movement covers the whole ventricular pressure decrement duration, is 33 ml/s for 60 bpm. The calculated speed by ABID is around 1.55 ml/s to 3.5 ml/s higher than the minimal ones. Therefore, the device successfully detects heart rate and calculates the suitable pacing speed for dilatation. This strategy demonstrates promising perspectives as a means to curtail the reliance on rapid ventricular pacing while maintaining hemodynamic stability during cardiac interventions.

Silicone aortic root phantoms were used to evaluate the dilatation performance. Silicone aortic valve models have been commonly used for investigating clinical techniques such as pressure drop estimations or training and simulation of surgical and endovascular interventions [26], [27]. The silicone (Dragon Skin 10) was selected for its mechanical similarity to native aortic valve leaflets [28], [29]. To mimic calcification, in previous studies, the use of thickened silicone leaflets has been attempted [30]. The employment of wax, with stiffness at the higher end of calcified tissue [31], provided a realistic approximation of calcified valves, resulting in systolic transvalvular gradients comparable to those seen in patients undergoing BAV [32], thus supporting the validity of the phantoms used in this study. The variation in wax distribution on the phantom led to marked differences in the pressure gradient. In Fig.4(e), calcified phantoms with a more significant accumulation of wax on the cusp of the leaflets exhibited a correspondingly higher pressure gradient.

The superior performance of balloon pacing is due to its higher radial pressure and precise synchronization with the cardiac cycle, allowing for more effective dilation during diastole when blood flow does not interfere. Measurements from rigid circular phantoms confirmed that the radial pressure applied by the pacing balloon exceeds that of traditional inflation methods. However, this increased pressure may limit its use in smaller implantation diameters, where internal balloon pressure approaches the burst threshold; therefore, the pacing approach was not tested on the 21 mm rigid annulus. Experimental results further demonstrate that balloon pacing at 60 bpm significantly outperforms the traditional dilatation method, achieving more significant TPG reductions and more substantial improvements in EOA. Specifically, balloon pacing reduced TPG by 27.09% (Cal2) and 30.28% (Cal4), compared to 15.04% (Cal1) and 17.03% (Cal3) with the traditional approach. Additionally, the higher radial pressure applied by the balloon facilitates greater leaflet separation, particularly in cases of severe calcification, where traditional methods may struggle to exert sufficient force. A previous study on balloon aortic valvuloplasty reports a reduction in systolic transvalvular gradients from 55 ± 21 mmHg to 29 ± 13 mmHg [32], similar to our results, indicating that our study reliably reflects expected in-vivo outcomes.

However, one of the limitations is that the suction in the syringe at 60 bpm causes the formation of significant amounts of vapour, which acts as a dampener and impedance, reducing and delaying the control of the balloon volume. Potential remedies include adjusting the aimed deflation volume below the 'safe' volume. Although the phantoms with similar wax distribution resulted in similar parameters, the slightly different wax accumulation might influence the result. Moreover, the calcified phantoms could not replicate the success of BAV reported in clinical reports, which is of at least a 30-40% decrease of TPG and/or $\geq$0.3 $cm^2$ increase in EOA [33], [15]. Despite the inherent fragility of wax, it may not entirely replicate the mechanical properties of actual leaflet calcification. Therefore, future work will include dilatation on the AR phantoms, which can have the ability of the reconfiguration to the original calcified distribution, fixed within the pulse duplicator under a fluidic environment aligning with the function of annular sizing (see our previous work [34]) and the use of novel materials to accurately mimic the mechanical properties of calcification.

## VI. Conclusion

We introduced an approach to BAV utilizing a valvuloplasty balloon catheter, with the core aim of minimizing reliance on RVP by synchronized balloon inflation and deflation aligned with the cardiac cycle. Specifically, it seeks to achieve expansion of calcified leaflets during the diastolic phase and deflate to a compact state before the systolic pressure increment, preserving the valve function and ensuring stability. Our method shows better dilatation performance, as evidenced by notable improvements in pressure gradient and aortic valve opening area. Importantly, this innovation serves to mitigate the complications associated with RVP during interventions, employing commercially available balloon catheters rather than novel research devices. It has the potential to improve the efficacy of BAV procedures, contributing to enhanced success rates. For more comprehensive validation, future investigations should consider implementing the balloon catheter within a pulse duplicator setup to achieve synchronization under realistic conditions. Furthermore, to provide a deeper understanding, future studies could delve into the intricate relationship between pacing speed

and dilatation performance. This exploration may encompass patient-specific models, considering varying calcification distributions on leaflets. Such advancements promise to refine BAV procedures and reduce associated risks.

## REFERENCES


[1] WHO. (2018) The top 10 causes of death. [Online]. Available: https://www.who.int/news-room/fact-sheets/detail/the-top-10-causes-of-death

[2] K. Amrit, J. T. Jeremy, and V. T. Nkomo, "Management of patients with aortic valve stenosis," *Mayo Clinic Proceedings*, vol. 93, no. 4, pp. 488–508, 2018.

[3] L. A. Goeddel, J. Serini, J. W. Steyn, A. S. Evans, S. Dwarakanath, H. Ramakrishna, J. Augoustides, and M. B. Brady, "Transcatheter aortic valve replacements: Current trends and future directions," *Seminars in Cardiothoracic and Vascular Anesthesia*, vol. 23, no. 3, pp. 282–292, 2019.

[4] T. R. Keeble, A. Khokhar, M. M. Akhtar, A. Mathur, R. Weerackody, and S. Kennon, "Percutaneous balloon aortic valvuloplasty in the era of transcatheter aortic valve implantation: a narrative review," *Open Heart*, vol. 3, no. 2, p. e000421, 2016.

[5] I. Daehnert, C. Rotzsch, M. Wiener, and P. Schneider, "Rapid right ventricular pacing is an alternative to adenosine in catheter interventional procedures for congenital heart disease," *Heart*, vol. 90, no. 9, pp. 1047–1050, 2004.

[6] C. Witzke, C. W. Don, R. J. Cubeddu, J. Herrero-Garibi, E. Pomerantsev, A. Caldera, D. McCarty, I. Inglessis, and I. F. Palacios, "Impact of rapid ventricular pacing during percutaneous balloon aortic valvuloplasty in patients with critical aortic stenosis: should we be using it?" *Catheterization and Cardiovascular Interventions*, vol. 75, no. 3, pp. 444–452, 2010.

[7] B. M. Jones, Y. Jobanputra, A. Krishnaswamy, S. Mick, M. Bhargava, B. L. Wilkoff, and S. R. Kapadia, "Rapid ventricular pacing during transcatheter valve procedures using an internal device and programmer: A demonstration of feasibility," *Catheterization and Cardiovascular Interventions*, vol. 95, no. 5, pp. 1042–1048, 2020.

[8] A. Shivaraju, C. Thilo, N. Sawlani, I. Ott, H. Schunkert, W. Von Scheidt, A. Kastrati, and A. M. Kasel, "Aortic Valve Predilatation with a Small Balloon, without Rapid Pacing, prior to Transfemoral Transcatheter Aortic Valve Replacement," *BioMed Research International*, vol. 2018, no. February 2014, pp. 2–7, 2018.

[9] S. Toggweiler, L. Loretz, M. Brinkert, M. Bossard, M. Wolfrum, F. Moccetti, B. Berte, F. Cuculi, and R. Kobza, "Simplifying transfemoral acurate neo implantation using the trueflow nonocclusive balloon catheter," *Catheterization and Cardiovascular Interventions*, vol. 96, no. 6, pp. E640–E645, 2020.

[10] J. Yao, G. M. Bosi, G. Burriesci, and H. Wurdemann, "Computational analysis of balloon catheter behaviour at variable inflation levels," in *International Conference of the IEEE Engineering in Medicine & Biology Society*, 2022, pp. 3015–3019.

[11] B. Faurie, M. Abdellaoui, F. Wautot, P. Staat, D. Champagnac, J. Wintzer-Wehekind, G. Vanzetto, B. Bertrand, and J. Monségu, "Rapid pacing using the left ventricular guidewire: reviving an old technique to simplify bav and tavi procedures," *Catheterization and Cardiovascular Interventions*, vol. 88, no. 6, pp. 988–993, 2016.

[12] C. Tumscitz, "Balloon aortic valvuloplasty through radial access," pp. 28–30, 2021.

[13] B. R. Lindman, M.-A. Clavel, P. Mathieu, B. Iung, P. Lancellotti, C. M. Otto, and P. Pibarot, "Calcific aortic stenosis," *Nature Reviews. Disease Primers*, vol. 2, p. 16006, 2016.

[14] K. Piayda, A. C. Wimmer, H. Sievert, K. Hellhammer, S. Afzal, V. Veulemans, C. Jung, M. Kelm, and T. Zeus, "Contemporary use of balloon aortic valvuloplasty and evaluation of its success in different hemodynamic entities of severe aortic valve stenosis," *Catheterization and Cardiovascular Interventions*, vol. 97, no. 1, pp. E121–E129, 2021.

[15] ——, "Contemporary use of balloon aortic valvuloplasty and evaluation of its success in different hemodynamic entities of severe aortic valve stenosis," *Catheterization and Cardiovascular Interventions*, vol. 97, no. 1, pp. E121–E129, 2021.

[16] A. B. de Oliveira Moraes, B. E. Stähli, B. J. Arsenault, D. Busseuil, N. Merlet, C. Gebhard, A. Fortier, D. Rhainds, M.-P. Dubé, M.-C. Guertin *et al.*, "Resting heart rate as a predictor of aortic valve stenosis progression," *International Journal of Cardiology*, vol. 204, pp. 149–151, 2016.

[17] O. Bazan and J. P. Ortiz, "Duration of systole and diastole for hydrodynamic testing of prosthetic heart valves: comparison between iso 5840 standards and in vivo studies," *Brazilian Journal of Cardiovascular Surgery*, vol. 31, pp. 171–173, 2016.

[18] C. Tumscitz, "Balloon aortic valvuloplasty through radial access," *Cardiac Interventions Today*, vol. 15, no. 5, pp. 28–30, 2021.

[19] C. Tumscitz, G. Campo, M. Tebaldi, F. Gallo, L. Pirani, and S. Biscaglia, "Safety and feasibility of transradial mini-invasive balloon aortic valvuloplasty: a pilot study," *JACC: Cardiovascular Interventions*, vol. 10, no. 13, pp. 1375–1377, 2017.

[20] P. Pibarot and J. G. Dumesnil, "Improving assessment of aortic stenosis," *Journal of the American College of Cardiology*, vol. 60, no. 3, pp. 169–180, 2012.

[21] B. H. Grimard, R. E. Safford, and E. L. Burns, "Aortic stenosis: diagnosis and treatment," *American Family Physician*, vol. 93, no. 5, pp. 371–378, 2016.

[22] N. Saikrishnan, G. Kumar, F. J. Sawaya, S. Lerakis, and A. P. Yoganathan, "Accurate assessment of aortic stenosis: a review of diagnostic modalities and hemodynamics," *Circulation*, vol. 129, no. 2, pp. 244–253, 2014.

[23] P. Fefer, A. Bogdan, Y. Grossman, A. Berkovitch, Y. Brodov, R. Kuperstein, A. Segev, V. Guetta, and I. M. Barbash, "Impact of rapid ventricular pacing on outcome after transcatheter aortic valve replacement," *Journal of the American Heart Association*, vol. 7, no. 14, p. e009038, 2018.

[24] M. Kanchi and A. C. NV, "Intra-aortic balloon pump—current status," *Journal of Cardiac Critical Care TSS*, vol. 2, no. 02, pp. 071–078, 2018.

[25] J. Yao, J. Salmonsmith, G. M. Bosi, G. Burriesci, and H. Wurdemann, "Finite element and fluid-structure interaction modelling of a balloon catheter," *IEEE Transactions on Medical Robotics and Bionics*, vol. 6, no. 1, pp. 68–72.

[26] C. Dockerill, H. Gill, J. F. Fernandes, A. Q. Nio, R. Rajani, and P. Lamata, "Blood speckle imaging compared with conventional doppler ultrasound for transvalvular pressure drop estimation in an aortic flow phantom," *Cardiovascular Ultrasound*, vol. 20, no. 1, pp. 1–11, 2022.

[27] A. A. Lezhnev, D. V. Ryabtsev, D. B. Hamanturov, V. I. Barskiy, and S. P. Yatsyk, "Silicone models of the aortic root to plan and simulate interventions," *Interactive CardioVascular and Thoracic Surgery*, vol. 31, no. 2, pp. 204–209, 2020.

[28] Y. Chen, X. Lu, H. Luo, and G. S. Kassab, "Aortic leaflet stresses are substantially lower using pulmonary visceral pleura than pericardial tissue," *Frontiers in Bioengineering and Biotechnology*, vol. 10, p. 869095, 2022.

[29] J. Illi, M. Ilic, A. W. Stark, C. Amstutz, J. Burger, P. Zysset, A. Haeberlin, and C. Gräni, "Mechanical testing and comparison of porcine tissue, silicones and 3d-printed materials for cardiovascular phantoms," *Frontiers in Bioengineering and Biotechnology*, vol. 11, 2023.

[30] S. Wang, H. Gill, W. Wan, H. Tricker, J. F. Fernandes, Y. Noh, S. Uribe, J. Urbina, J. Sotelo, R. Rajani *et al.*, "Manufacturing of ultrasound-and mri-compatible aortic valves using 3d printing for analysis and simulation," in *Statistical Atlases and Computational Models of the Heart.*, 2020, pp. 12–21.

[31] E. A. Igwe and P. K. Fun-Akpo, "Evaluation of modulus of elasticity of candle wax modified hma concretes using hondros model from indirect tensile test," *International Journal of Constructive Research in Civil Engineering*, 2020.

[32] C. M. Otto, M. C. Mickel, J. W. Kennedy, E. L. Alderman, T. M. Bashore, P. C. Block, J. A. Brinker, D. Diver, J. Ferguson, and D. R. Holmes Jr, "Three-year outcome after balloon aortic valvuloplasty. insights into prognosis of valvular aortic stenosis," *Circulation*, vol. 89, no. 2, pp. 642–650, 1994.

[33] I. Ben-Dor, G. Maluenda, D. Dvir, I. M. Barbash, P. Okubagzi, R. Torguson, J. Lindsay, L. F. Satler, A. D. Pichard, and R. Waksman, "Balloon aortic valvuloplasty for severe aortic stenosis as a bridge to transcatheter/surgical aortic valve replacement," *Catheterization and Cardiovascular Interventions*, vol. 82, no. 4, pp. 632–637, 2013.

[34] J. Yao, G. M. Bosi, A. Palombi, G. Burriesci, and H. Wurdemann, "Compliant aortic annulus sizing with different elliptical ratios through a valvuloplasty balloon catheter," *IEEE Transactions on Biomedical Engineering*, vol. 70, no. 12, pp. 3469–3479.